UC Irvine
UC Irvine Previously Published Works

Title
Nonlinear optical diagnosis of oxide traps formed during reactive ion etching

Permalink
https://escholarship.org/uc/item/1893v84n

Journal
Journal of Applied Physics, 88(5)

ISSN
0021-8979

Authors
Fang, J
Heidbrink, WW
Li, GP

Publication Date
2000-09-01

DOI
10.1063/1.1288168

Copyright Information
This work is made available under the terms of a Creative Commons Attribution License, availalbe at https://creativecommons.org/licenses/by/4.0/

Peer reviewed

eScholarship.org Powered by the California Digital Library
University of California

Nonlinear optical diagnosis of oxide traps formed during reactive ion etching

J. Fang, W. W. Heidbrink,[a] and G. P. Li
University of California, Irvine, California 92697

(Received 22 February 2000; accepted for publication 7 June 2000)

Oxide traps generated by reactive ion etching are studied using a pulsed femtosecond laser. The second harmonic generation (SHG) signal from the Si/SiO_2 interface is sensitive to charged traps in the oxide. The time evolution of the SHG signal indicates that positive traps predominate. The angular dependence of the polarized signal shows that the electric field generated by the oxide traps alters the symmetry of the sample. The damage is greatest for an oxide thickness of 13 nm (for a plasma dc bias of 300 V). Thicker oxides have smaller SHG signals, presumably because the Fowler–Nordheim tunneling currents induced by plasma charging of the oxide surface are smaller. Very thin oxides also exhibit reduced damage. The time dependent SHG signals depend on the temperature of the samples; these data provide information on the trapping and detrapping of substrate electrons by oxide holes. © *2000 American Institute of Physics.*
[S0021-8979(00)02918-2]

I. INTRODUCTION

When exposed directly to a plasma, a wafer with a thin oxide is subject to two major kinds of damage. Bombardment by electrons, ions, atoms, radicals, and ultraviolet radiation cause damage to the exposed oxide,[1] while surface charging produces indirect damage.[2] The surface charging occurs when the electron and ion currents that flow from the plasma source to the wafer do not balance locally. As the charge builds up on the wafer surface, the voltage across the dielectric layer (gate oxide) increases until the oxide layer starts to conduct via a Fowler–Nordheim (FN) tunneling current. Both direct and indirect damage create trapped charges inside the oxide bulk and at the Si/SiO_2 interface. Trapped charges affect the dielectric properties of the device and therefore adversely impact the yield and reliability of metal-oxide-semiconductor (MOS) transistors in very large scale integration production. New diagnostics of charge trapping can enhance our understanding of degradation at the Si/SiO_2 interface and in the oxide bulk, provide improved process control, and aid the development of the next generation of plasma reactors.

The role of FN stress in oxide damage is well established,[2] but many details remain unresolved. Spatial variations in surface charging correlate with the location of damage.[3] Although the plasma parameters oscillate at the radio frequency of the plasma source, it is the average imbalance between the ion and electron currents that is responsible for surface charging.[4] Once the surface charges, the dc sheath current through the plasma and the FN current through the oxide are equal.[4,5] The damage depends on oxide thickness, with a 12-nm-thick oxide suffering greater damage than thicker or thinner oxides.[5] In oxides that are too thick to support appreciable FN currents, exposure to UV light creates positive trapping sites in the oxide.[6] Under these circumstances, the positive holes accumulate near the Si/SiO_2 interface.[7]

Traditional techniques for the study of gate oxide damage can be categorized as source measurements or result measurements. Source measurements diagnose the charge buildup or the plasma uniformity to indicate potential hardware problems. Measuring the threshold voltage shifts of MOS capacitor or *n*-channel MOS transistors is the conventional way to determine the charge buildup;[8] however, to determine the distribution of peak surface potential across the wafer requires fabrication of such devices throughout the entire wafer. Langmuir probes can measure the plasma potential[3] but the technique is difficult to implement on most commercial etching equipment. Measurements of the results of oxide damage are even more problematic. Measurements of the threshold voltages require fabrication of an antenna structure or large area capacitor over the gate electrode. Unfortunately, a large polysilicon antenna is perturbative: the structure blocks ultraviolet radiation and inhibits annealing.[9] Damage measurements in fully covered MOS capacitors may be inaccurate[6]. In this article, we show that a nonlinear optical probe, the second harmonic generation (SHG) signal from the SiO_2/Si interface, provides a nonperturbative diagnostic of charge trapping caused by plasma etching. The technique is sensitive to both radiation-induced damage and to damage caused by FN tunneling. Our results suggest that both FN currents and UV exposure play important roles in oxide damage during reactive ion etching (RIE).

The article is organized as follows. Section II describes the diagnostic technique and measurements that demonstrate that SHG is sensitive to oxide damage. Measurements of the plasma-induced damage as a function of oxide thickness are presented and interpreted in Sec. III. Section IV discusses the time dependence of the SHG signals; these measurements indicate that the oxide holes are predominately positively charged. The charge state of the trapping sites depends on the oxide temperature (Sec. V). The implications of these

[a]Electronic mail: wwheidbr@uci.edu

 © 2000 American Institute of Physics

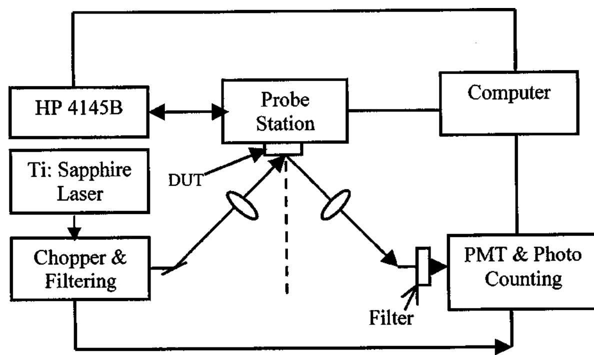

FIG. 1. Schematic diagram of the apparatus used to study the device under test.

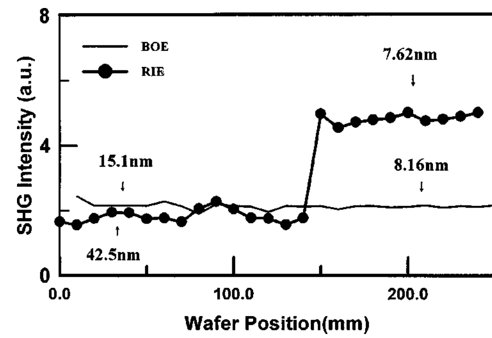

FIG. 2. Comparison of the SHG signals from RIE and BOE processed samples. When the laser scans across the chemically etched region the SHG signal is unchanged, but the signal is significantly enhanced in the sample that was processed by the plasma.

results are discussed in Sec. VI and the conclusions appear in Sec. VII.

II. EXPERIMENTAL TECHNIQUE AND BASIC MEASUREMENTS

When illuminated by an intense laser beam of frequency ω, a nonlinear dielectric medium can radiate light of frequency 2ω, a process known as SHG. In a centrosymmetric medium such as silicon, SHG occurs primarily at the interface where the symmetry is broken[10]. A static electric field across the interface also alters the symmetry and therefore modifies the intensity of the SHG signal. Both externally imposed dc fields[11] and fields produced by trapped charges[12] affect the SHG signal.

A schematic of the experiment is shown in Fig. 1. The fundamental light source is a Ti:sapphire laser pumped by a pointing-stabilized mode-locked Nd:yttrium–aluminum–garnet laser.[13] The laser produces 50 fs pulses at a wavelength of 800 nm, a repetition rate of 78 MHz, and an average power of 200 mW. The p-polarized laser beam is focused at a 45° incident angle onto a 6 μm diameter spot on the processed Si/SiO_2 sample. The reflected, filtered, p-polarized second harmonic light is collected by a photomultiplier and lock-in amplifier gated by a 1 kHz chopper. The sample rests in air on a computer controlled rotational stage that records interface SHG intensities as a function of azimuthal angle and translational position of the sample.

Samples are cut from a p-type (100) silicon wafer with a thermally grown oxide of 70 nm. Using a Plasma-Therm 790 series parallel plate RIE etcher, which is a typical commercial nonmagnetic plasma system, a series of oxide films are etched to different thicknesses with a CHF_3/O_2 mixture at a chamber pressure of 40 mTorr. The dc bias voltage ranges from 300 to 400 V.

Plasma processing has a stronger effect on the SHG signal than wet chemical etching, as illustrated in Fig. 2. In this comparison, an unmasked portion of the sample was etched either by RIE or by buffered oxide etch (BOE), then the SHG signal was measured as a function of position on the sample. In the case of plasma processing, the SHG signal is 2.6 times larger when the laser probes the thin portion of the sample while, for wet chemical etching, the SHG signal is unchanged by the etching process. Evidently, plasma processing creates additional trapped charge in the sample, thereby altering the electric field at the interface.

More detailed information about the origin of these changes is given by the angular dependence of the SHG signal. It is well established both theoretically[14] and experimentally[15] that the SHG signal from a cubic silicon crystal has both an isotropic and anisotropic component. In a pure Si(100) crystal with a uniform oxide layer, the expected second-harmonic electric field[14] is proportional to $a_{pp} + c_{pp}\cos(4\phi)$, where a_{pp} and c_{pp} are constants and ϕ is the angle between the crystal face and the direction of SHG propagation. The expected SHG intensity is therefore

$$I \propto [a_{pp} + c_{pp}\cos(4\phi)]^2. \qquad (1)$$

Figure 3(a) shows the SHG signal as a function of azimuthal angle ϕ for a 70 nm, thermally grown oxide on the (100) silicon surface (prior to any plasma processing). The signal clearly shows the expected four-fold, $\cos(4\phi)$, contribution. The theoretical prediction [Eq. (1)] provides an excellent fit to the data. Next, this same sample is etched by the plasma

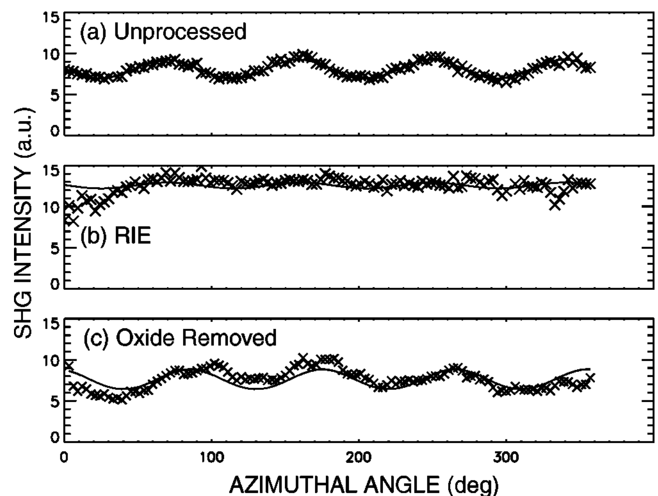

FIG. 3. The dependence of the SHG signal on rotational angle for (a) thermally grown oxide on silicon, (b) the same oxide after plasma processing and (c) the same sample after BOE wet chemical removal of the RIE etched oxide layer. The solid lines show the best least-squares fits to the theoretical model of Eq. (1). (a) $a_{pp}=2.84$; $c_{pp}=0.20$. (b) $a_{pp}=3.55$; $c_{pp}=0.05$. (c) $a_{pp}=2.75$; $c_{pp}=0.22$.

down to an oxide thickness of 12.7 nm and the measurement is repeated. Now the isotropic component of the signal is 50% larger and the $\cos(4\phi)$ anisotropic component is almost completely eliminated [Fig. 3(b)]. Finally, the remaining oxide is removed by wet chemical etching and the measurement is repeated once again [Fig. 3(c)]. With the oxide removed, the four-fold symmetry is recovered and the coefficients a_{pp} and c_{pp} are similar to the initial values for the unprocessed oxide, but the deviations from the theoretical model are larger.

The data in Fig. 3(b) are unusual. In previous nonlinear studies of electroreflectance in silicon and metals[11] the dc bias field changes both the magnitude and the phase angle of the ratio between isotropic and anisotropic contributions, but the four-fold anisotropy pattern remains. Since the four-fold pattern returns when the oxide is removed, we know that the altered symmetry is caused by changes in the oxide (not the silicon). We postulate that trapped charge sites have a nonuniform distribution in the oxide so that the isotropic second-harmonic polarization changes inhomogeneously (laterally); the electric fields from these randomly distributed charges add incoherently, increasing the isotropic SHG signal but canceling the constructive interference between the isotropic and anisotropic contributions that generates the four-fold symmetry.

III. DEPENDENCE OF THE OXIDE TRAP DENSITY ON OXIDE THICKNESS

An urgent concern in the design of future silicon devices is the viability of extremely thin oxide layers. In this section, we measure plasma-induced oxide damage as a function of oxide depth and interpret the results with a simple model.

We prepare Si/SiO_2 samples under three different plasma conditions. In each case, a 70 nm oxide is etched by a CHF_3/O_2 mixture down to a variety of remaining thicknesses. The plasma dc bias voltage is either 300, 350, or 400 V. Each sample is then scanned by the laser. The interface SHG signal intensities, I/I_0, are plotted as a function of the thickness of the remaining oxide layer in Fig. 4. Here, I is the SHG signal from the etched sample and I_0 is the SHG signal from an unetched control sample. A significant enhancement of SHG signal from the original fresh oxide signal level is observed at a threshold etched oxide thickness of about 30 nm. The SHG signal steadily increases as the oxide thickness is further reduced until a maximum is observed in the range of 13–18 nm. The maximum signal occurs at larger values of oxide thickness for higher values of plasma dc bias voltage (Fig. 5). For thinner oxides, the SHG signal steadily decreases. Finally, when the oxide layer on the silicon substrate is nearly removed the SHG intensity is comparable to the SHG intensity of the control.

To understand the SHG intensity dependence on the oxide thickness, we adopt the model of Shin *et al.*[5] In steady state, net charge does not accumulate so the average current flow is divergence free. Consider the surface of the oxide. At this location, there are three contributions to the current: the ion current across the plasma sheath I_i, the electron current across the plasma sheath I_e, and the current that flows through the oxide I_{FN}. The ion current I_i is insensitive to the actual value of the potential difference across the sheath, $V_p - V_{ox}$, and can be taken as a constant. Here V_p is the average plasma potential and V_{ox} is the average voltage at the front surface of the oxide (both measured relative to the silicon wafer). The sheath potential opposes electron flow, however, so electrons only flow from the plasma to the oxide when their kinetic energy exceeds the potential energy ''hill.'' The net current to the plasma I_p is therefore given by the Langmuir-probe I–V characteristics

$$I_p = I_{e0} \exp[-e(V_p - V_{ox})/kT_e] - I_i. \quad (2)$$

Here I_{e0} is the magnitude of electron current at $V_p - V_{ox} = 0$ and T_e is the electron temperature of the plasma. Consider first a thick oxide. According to Eq. (2), the sheath voltage $V_p - V_{ox}$ adjusts until the plasma electron current balances the plasma ion current and $I_p = 0$. Because the oxide is thick, current neutrality is obtained without a large

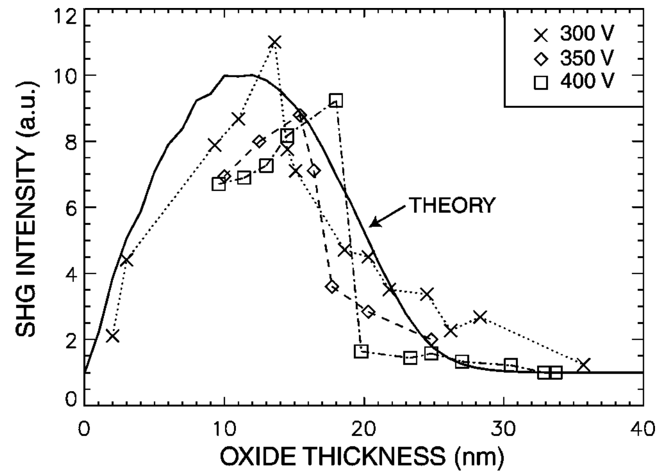

FIG. 4. Normalized SHG intensity as a function of oxide thickness for samples processed at three different values of plasma dc bias. The solid curve is the theoretically predicted variation of I_pT_{ox} for $I_{e0}/I_i = 20$, $T_e = 6.8$ V, $V_p = 25$ V, and $B = 250$ V/nm.

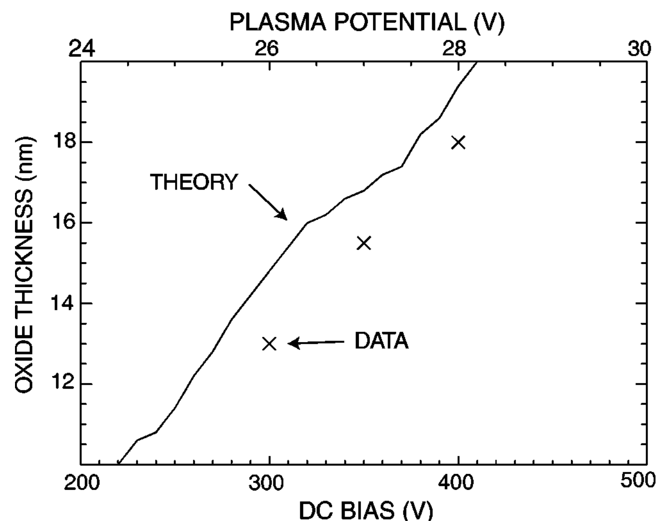

FIG. 5. Thickness of oxide at maximum SHG signal versus plasma dc bias (x) for the data of Fig. 4. The solid line is the thickness at the calculated maximum of I_pT_{ox} as a function of the plasma potential V_p. ($I_{e0}/I_i = 20$; $T_e = 6.8$ V; $B = 250$ V/nm.)

electric field appearing across the oxide; in other words, the FN turn-on voltage is too high in a thick oxide for appreciable current to flow. Since no current flows through the oxide, no current-induced damage occurs. (Direct damage caused by radiation is still operative, however.) This explains why the SHG signal approaches that of the control ($I/I_0 \rightarrow 1$) for oxide thicknesses larger than 30 nm. In contrast, in a thinner oxide, the oxide electric field is larger and a FN tunneling current begins to flow through the oxide before the sheath potential is small enough to allow a neutralizing electron current from the plasma. The FN tunneling current is given by

$$I_p = A(V_{ox}/T_{ox})^2 \exp(-BT_{ox}/V_{ox}), \tag{3}$$

where T_{ox} is the oxide thickness and A and B are constants. In steady state, the net plasma current [Eq. (2)] equals the FN tunneling current [Eq. (3)]. The simultaneous solution of Eqs. (2) and (3) predicts that the FN tunneling current increases rapidly as the oxide thickness T_{ox} is decreased. Since oxide damage is caused by microscopic processes, the *density* of trapping sites is expected to depend on the current density J. The larger FN current creates more trapping sites in the oxide, resulting in a larger SHG signal.

In this model, the FN tunneling current continues to increase as the oxide thickness is further reduced. On the other hand, the expected SHG signal does not continue to increase. As discussed in Sec. II, trapped charge throughout the oxide contributes to the electric field at the interface and affects the SHG signal. Thus, the SHG signal is expected to depend upon the total *number* of trapped charges in the oxide. In the limit of *vanishing* oxide, the FN tunneling current remains finite[5], so the number of trapped charges decreases in an ultrathin oxide. As the oxide thickness shrinks to zero, the SHG signal is due exclusively to the silicon interface, so the intensity should equal the intensity of an undamaged control. In mathematical language, we expect $I \rightarrow I_0$ as $T_{ox} \rightarrow 0$.

As shown in Fig. 4, this model explains the thickness dependence of the SHG signal. The agreement with the model is only qualitative, not quantitative, for two reasons. First, the actual values of the parameters in Eqs. (2) and (3) are uncertain and the shape of the curve is quite sensitive to the assumed values of these parameters (although we have used plausible values). Second, the SHG signal is assumed proportional to $I_p T_{ox}$, which is an oversimplified description of trapped-charge creation and of the resulting SHG intensity.[16] Nevertheless, the general features of the data are satisfactorily reproduced by the model.

With the plausible assumption that the plasma potential becomes larger when the dc bias voltage increases,[17] this model also successfully predicts that the maximum SHG signal should shift to larger thicknesses at large bias voltage, as experimentally observed (Fig. 5).

IV. TIME DEPENDENCE OF THE SHG SIGNAL

In addition to probing the electric field at the interface, laser illumination can inject electrons into the oxide, thereby altering the state of the trapping sites. The data in the previous sections are initial SHG measurements, acquired before injected electrons have altered the sample. In this section, the time evolution of the SHG signal under conditions of constant laser illumination are examined.

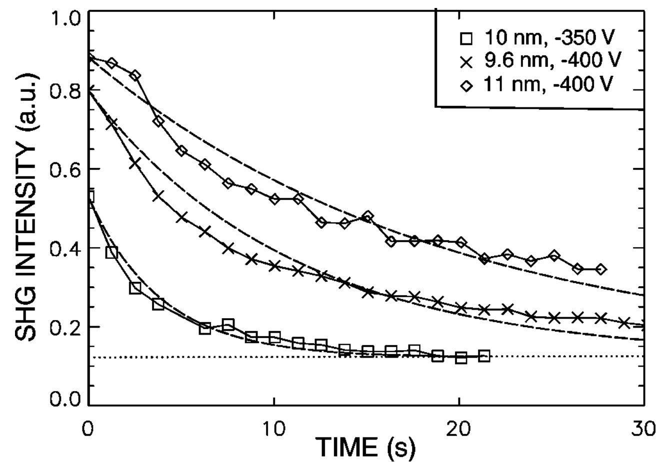

FIG. 6. Time dependent SHG signal from three RIE etched samples. The dashed lines are the exponential decays predicted by the constant probability model for values of $1/\nu$ of 3.9, 11, and 19 s, respectively.

The SHG signal from samples that have been etched by a plasma decreases in time, as shown in Fig. 6. Under constant illumination, the SHG signal steadily approaches the signal level of the unetched control samples on a 10 s timescale. More extensively damaged samples (ones with larger initial SHG signals) return to the baseline level more slowly than less damaged samples.

The SHG signals in Fig. 6 decay approximately exponentially. The measured curves I are conveniently parameterized by $I - I_0 = \Delta I \exp(-\nu t)$, where I_0 is the control SHG signal, ΔI is a constant, and ν is the decay rate. The measured decay rates for dc biases of 300–400 V and oxide thicknesses of 9-31 nm are summarized in Fig. 7. The signal decays in a few seconds for barely damaged samples ($I/I_0 \simeq 2$) but takes minutes to return to the control level for severely damaged samples ($I/I_0 \simeq 10$). For the same level of initial damage, thinner samples decay more rapidly than

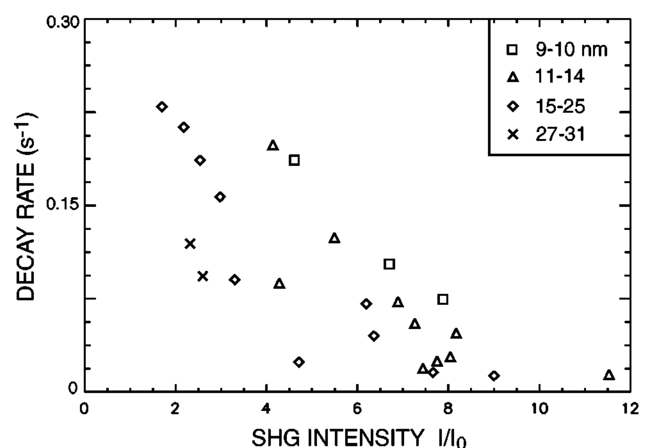

FIG. 7. Dependence of the decay rate ν on the initial, normalized SHG intensity for RIE processed samples of various oxide thicknesses between 9 and 31 nm.

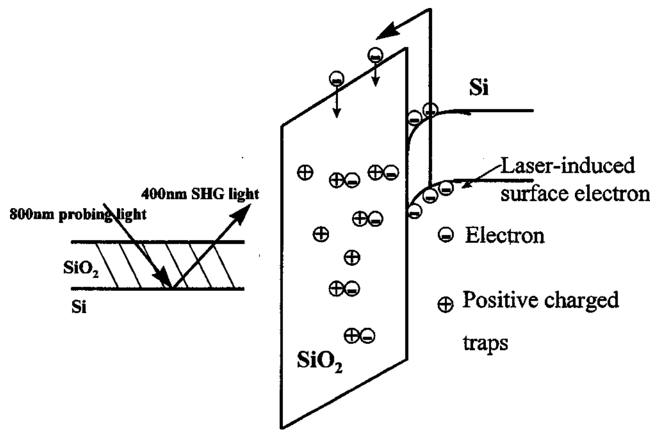

FIG. 8. Schematic diagram of the neutralization of positive traps by laser-injected electrons.

thicker samples. As discussed in Sec. III, the dc bias affects the signal level but, apart from its effect on I/I_0, the dc bias has little effect on the decay rate.

The data in Figs. 6 and 7 demonstrate that the trapping sites produced by the plasma are positive oxide traps. When the silicon wafer is illuminated with laser pulses at a high peak power of 10 $\mathrm{GW/cm^{-2}}$, substrate electrons are pumped into the oxide layer through multiphoton absorption[18] (Fig. 8). These electrons neutralize the positive charged traps in the oxide, thereby reducing the local electric field and causing a reduction in SHG signal. It is important to note that samples that are subjected to FN stress in the absence of plasma behave in the *opposite* manner: the SHG signal *increases* in time as the neutral oxide traps gradually charge negatively[12]. The decaying SHG signals in Fig. 6 show that laser-injected electrons alter positive traps more rapidly than neutral traps in plasma-processed samples.

A simple model predicts exponential decay of the signals. Presumably, electrons are injected into the oxide at a constant rate by the laser. For simplicity, assume that the SHG signal is linearly proportional to the number of positive traps in the oxide N_p. If the probability of neutralization is proportional to the number of traps (as would be expected if few injected electrons recombine), then the expected behavior of the SHG signal I is

$$\frac{dI}{dt} \propto \frac{dN_p}{dt} = -\nu N_p, \tag{4}$$

which implies exponential decay of the SHG signal, $I \propto \exp(-\nu t)$. This ''constant probability'' model provides a fair description of the time evolution of the SHG signal (Fig. 6). The smaller value of ν for thicker oxides (Fig. 7) probably indicates that injected electrons are less likely to neutralize distant positive traps in a thick oxide. Closer inspection of the fits in Fig. 6 shows that early data points fall below the fitted curve while later ones lie above it; in other words, the initial decay proceeds more rapidly than the later decay. This may indicate that some traps have a higher probability of neutralization than others, perhaps due to varying distances from the interface.

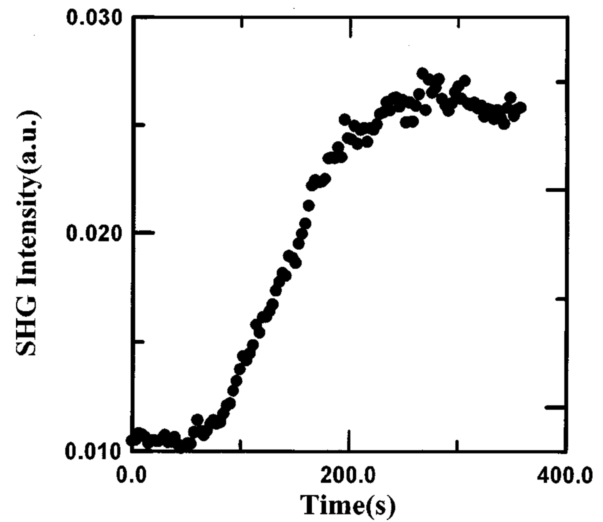

FIG. 9. SHG signal vs time during constant laser illumination for a sample that is heated from room temperature to 110 °C.

V. TEMPERATURE DEPENDENCE OF THE TIME DEPENDENT SHG SIGNAL

When a RIE etched sample is exposed to constant laser illumination, the SHG signal gradually decreases, as discussed in the previous section. When an illuminated sample is subsequently heated from room temperature to 110 °C, re-emission of captured electrons from the hole traps is observed (Fig. 9). After the sample temperature reaches 110 °C, the SHG intensity increases slowly and returns to the initial signal level (prior to either laser illumination or heating). It takes more than 100 s for the SHG intensity to recover, suggesting that the release of electrons from the positive trap sites takes much longer than their initial capture by laser-induced electron injection.

The temperature dependence of this reemission process is shown in Fig. 10(a). At 50 °C, only partial recovery of the

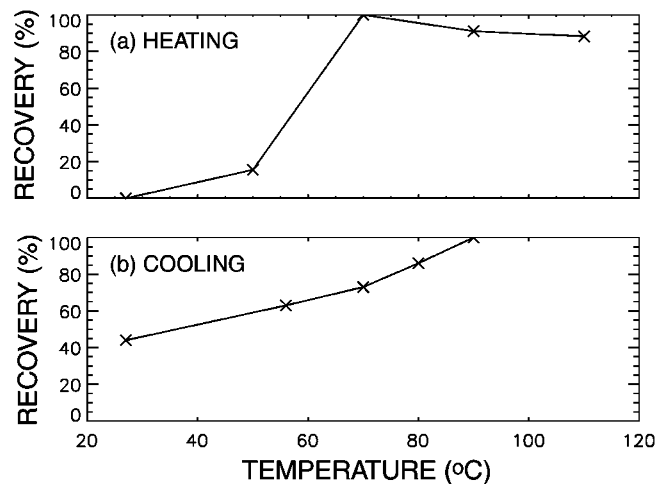

FIG. 10. Change in steady-state SHG signal vs sample temperature for (a) samples heated from room temperature and (b) samples cooled from 130 °C. The recovery is defined as $(I-I_\infty)/(I_0-I_\infty)$, where I is the SHG intensity at the elevated temperature, I_0 is the initial SHG signal at room temperature, and I_∞ is the room temperature SHG signal after laser illumination.

initial SHG signal is observed. For temperatures of 70 °C and above, essentially complete recovery occurs. As expected, the SHG signal never exceeds the initial level because the thermal energy ionizes existing positive traps but cannot create any new traps.

If the heated sample is subsequently cooled, the SHG signal decreases again, but hysteresis is observed. Figure 10(b) shows the dependence of the SHG intensity on the sample temperature when the sample temperature decreases from 130 °C to a lower temperature. As the sample temperature decreases (during constant laser illumination), the SHG signal decreases, indicating reneutralization of some of the positive traps. However, at a given temperature, the SHG signal is larger during cooling [Fig. 10(b)] than the signal during heating [Fig. 10(a)]. This hysteresis indicates that the electron trapping probability by RIE-induced trap states depends on the sample's temperature history.

VI. MECHANISM OF RIE-INDUCED DAMAGE

In this section, we use the results of Secs. II–V to infer the nature of the RIE-induced damage.

The data in Secs. II–V are very different than the results of earlier SHG experiments with unetched samples.[18] In these earlier studies, the initial SHG signal was independent of oxide thickness; RIE-processed samples exhibit a strong dependence on thickness (Fig. 4). For an unetched sample, the time-dependent SHG signal increases during laser illumination; the SHG signal decays for RIE-processed samples (Fig. 6). For unetched samples, the thinnest samples exhibit the greatest change in time-dependent signal; for RIE-processed samples the change is greatest for intermediate thicknesses (Fig. 7). In Ref. 18, it is suggested that a surface effect involving the ambient oxygen is responsible for the observed behavior in unetched samples. The different behavior in our experiments suggests that bulk trapping effects are of greater importance in RIE-processed samples.

Our samples are subject to radiation-induced damage and current-induced damage. In Sec. III, we showed that a simple model of FN tunneling currents explains the observed dependence of SHG signal on oxide depth. In contrast, it is difficult to attribute the depth dependence to radiation damage. Consider first UV radiation. UV radiation of an oxide film can cause positive charge trapping,[7] which is consistent with the time evolution of the signal (Sec. IV). On the other hand, the most intense emission lines (114.9 and 130.5 nm for CHF_3 and O_2) are absorbed near the surface of the oxide film. Thus, one expects a weak dependence of SHG signal on oxide depth for direct UV-induced damage.

Another possible mechanism of positive trap formation is ion implantation by the plasma. Implanted ions could easily form positive traps. The maximum range of hydrogen ions for our conditions is 10–20 nm, with most ions deposited closer to the surface.[19,20] For this damage mechanism, one therefore expects an initial rise in SHG signal when the oxide is etched from 70 nm down to ~50 nm (as the implanted ions accumulate), then a relatively constant SHG signal until the oxide is 10–20 nm thick. In reality, however, strong variation in SHG signal is observed for thicknesses between 20 and 40 nm, so ion implantation is not the dominant cause of damage.

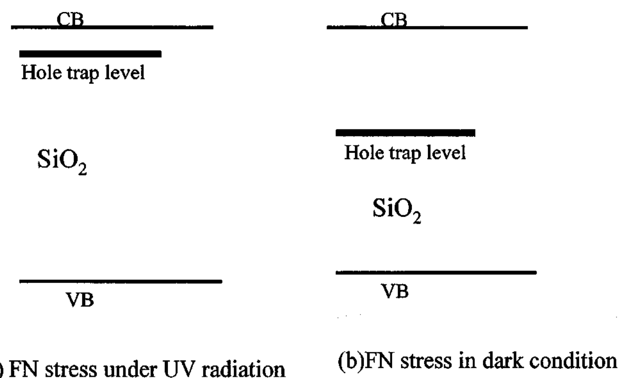

FIG. 11. Energy gap level diagram for hole traps created by (a) combined FN stress and UV radiation and (b) dark FN stress. The higher energy trap is more likely to be positively charged and is more sensitive to heating.

A simple, spatially uniform, model of FN tunneling adequately explains the dependence of SHG signal on oxide thickness (Sec. III). Extensions of this model that include spatial uniformities, such as the model discussed by McVittie,[2] could also explain the observed experimental trends.

The trapping sites are distributed throughout the oxide. Recall that all of our samples are initially thick (prior to etching). If the majority of created traps accumulated near the interface, they would not be removed by subsequent etching; hence, one would expect the largest SHG signal in the *thinnest* samples. Since, in fact, ~13 nm samples have much larger SHG signals than ultrathin samples, we conclude that most charge traps are removed when a sample is etched from 13 to 2 nm. Further evidence that the traps are distributed throughout the oxide is found in Fig. 7. Electrons that are injected across the interface by the laser neutralize charge traps more quickly in thin samples than in thick samples; if the trapping sites were concentrated near the interface, the decay rate would be independent of sample thickness.

The data in Fig. 4 corroborate earlier studies[21,22] that show ultrathin oxides can be processed without suffering extensive damage.

Although FN tunneling currents can explain the observed depth dependence of the SHG signal (Fig. 4), it is not obvious why the traps are positively charged. The traps are negatively charges in RIE-processed samples that are covered by an antenna.[23] Similarly, samples subjected to direct FN tunneling currents *in the dark* develop primarily negative and neutral traps.[12] Also, heating these samples to ~100 °C has little effect on the average charge state, while heating plasma-damaged samples to 100 °C has a dramatic effect (Sec. V). Evidently, the combination of FN stress and irradiation that occurs during RIE generates different trap sites than FN stress alone.

One possibility is that UV-induced electron-hole pairs participate in the FN tunneling and create a positive oxygen vacancy with a relatively shallow energy well (Fig. 11). In the case of dark FN stress, accelerated electrons and holes

break the Si–O bond creating oxygen vacancies; these O vacancies capture holes and distort the lattice structure.[24] Then this structure captures an electron and forms a neutral trap. During laser irradiation, some of these neutral trap sites capture laser-injected electrons and become negatively charged. These neutral traps are at an energy level far from the conduction band of SiO_2 and remain stable during heating. In contrast, when unpatterned oxide wafers are exposed directly to plasma during RIE processing, the FN tunneling current through the oxide consists of both UV-generated electron-hole pairs and conductors from the substrate. The UV-generated holes can have larger energies than holes generated by FN stress alone. The hole-trap oxygen vacancies created by these more energetic conductors have a gap level close to the conduction band of SiO_2. This higher gap level allows the O vacancy to capture and release electrons to the conduction band. These shallow traps remain positively charged at room temperature, capture laser-injected electrons during laser irradiation, but release captured electrons to the conduction band during heating.

It has been reported that UV light of energy greater than 4.3 eV (the energy barrier between Si and SiO_2) can cause electron injection from the substrate into the oxide layer and thus anneal the positive trapped charge near the interface.[9] In our experiment, however, the oxide is fully exposed to UV radiation so annealing should be operative, but complete annealing of the oxide trapped charges is not observed.

VII. CONCLUSIONS

SHG is a sensitive technique for the study of oxide damage caused by plasma processing. Conceivably, SHG could be employed as a noninvasive, real-time diagnostic during RIE.

The angular dependence of the SHG signal indicates that the plasma-induced oxide traps alter the symmetry of the sample.

Plasma-induced damage is greatest for oxide thicknesses of ~ 15 nm. Thicker oxides suffer less damage because little current flows through the sample. In thin oxides, the current is large but the current path is short.

The steady decrease of the SHG signal from an illuminated sample demonstrates that positive traps predominate. The neutralization of the positive traps proceeds more slowly in heavily damaged samples.

Neutralization of the positive traps by the laser can be reversed by heating the sample to 70 °C. The thermal history of the sample affects the number of positive traps.

[1] L. M. Ephrath, Solid State Technol. **25**, 87 (1982).
[2] J. P. McVittie, Tech. Dig. Int. Electron Devices Meet. 433 (1997).
[3] C. Cismaru, J. L. Shohet, K. Nauka, and J. B. Friedman, Appl. Phys. Lett. **72**, 1143 (1998).
[4] C. T. Gabriel and J. P. McVittie, Solid State Technol. **35**, 81 (1992).
[5] H. Shin, K. Noguchi, and C. Hu, IEEE Electron Device Lett. **14**, 509 (1993).
[6] S. P. Ashburn, S. Krishnan, G. A. Dixit, M. Rodder, K. Taylor, T. Breedijk, I.-C. Chen, M. W. Goodwin, and A. L. Esquivel, Tech. Dig. Int. Electron Devices Meet. 449 (1997).
[7] T. Yunogami, T. Mizutani, K. Suzuki, and S. Nishimatsu, Jpn. J. Appl. Phys., Part 1 **28**, 2172 (1989).
[8] C. T. Gabriel, J. Vac. Sci. Technol. B **9**, 370 (1991).
[9] K. Lai, K. Kumar, A. Chou, and J. C. Lee, IEEE Electron Device Lett. **17**, (1990).
[10] Y. R. Shen, Appl. Phys. A: Solids Surf. **59**, 541 (1994).
[11] J. I. Dadap, X. F. Hu, M. H. Anderson, and M. C. Downer, Phys. Rev. B **53**, R7607 (1996).
[12] J. Fang and G. P. Li, Appl. Phys. Lett. **75**, 3506 (1999).
[13] C. W. Siders, E. W. Gaul, M. C. Downer, A. Bibine, and A. Stepanov, Rev. Sci. Instrum. **65**, 3140 (1994).
[14] J. E. Sipe, D. J. Moss, and H. M. van Driel, Phys. Rev. B **35**, 1129 (1987).
[15] J. A. Litwin, J. E. Sipe, and H. M. van Driel, Phys. Rev. B **31**, 5543 (1985).
[16] For example, one deficiency of the model is that, as a sample is etched, damage should accumulate, i.e., the damage created in a thicker oxide is added to that created in a thinner oxide. Inclusion of this effect in the modeling does not alter the qualitative shape of the prediction, however. Since the FN current is much larger near the endpoint than in the thicker oxide, the accumulated damage $\int_{70\ \mathrm{nm}}^{T_{\mathrm{ox}}} I_p(T')\, dT'$ is similar in shape to the endpoint damage $I_p(T_{\mathrm{ox}})$.
[17] J. W. Coburn and E. Kay, J. Appl. Phys. **43**, 4965 (1972).
[18] J. Bloch, J. G. Mihaychuk, and H. M. van Driel, Phys. Rev. Lett. **77**, 920 (1996).
[19] G. S. Oehrlein, R. M. Tromp, J. C. Tsang, Y. H. Lee, and E. J. Perillo, J. Electrochem. Soc. **132**, 1441 (1985).
[20] G. S. Oehrlein, Phys. Today **39**, 26 (1986).
[21] H. S. Momose, S.-I. Nakamura, T. Ohguro, T. Yoshitomi, E. Morifuji, T. Morimoto, Y. Katsumata, and H. Iwai, Tech. Dig. Int. Electron Devices Meet. 453 (1997).
[22] S. Krishnan, S. Rangan, S. Hattangady, G. Xing, K. Brennan, M. Rodder, and S. Ashok, Tech. Dig. Int. Electron Devices Meet. 445 (1997).
[23] K. Noguchi, K. Takashiki, T. Horiuchi, and H. Miyamoto, Tech. Dig. Int. Electron Devices Meet. 441 (1997).
[24] A. Yokozawa, A. Oshiyama, Y. Miyamoto, and S. Kumashiro, Tech. Dig. Int. Electron Devices Meet. 703 (1997).